Geophys. J. Int. (2001) **147,** 630–638

Crustal model for the Middle East and North Africa region: implications for the isostatic compensation mechanism

Dogan Seber, Eric Sandvol, Christine Sandvol, Carrie Brindisi and Muawia Barazangi

Institute for the Study of the Continents, Cornell University, Ithaca, NY 14853, *USA. E-mail: seber@geology.cornell.edu*

Accepted 2001 August 13. Received 2001 August 6; in original form 2001 March 16

SUMMARY

We present a new 3-D crustal model for the Middle East and North Africa region that includes detailed topography, sediment thickness, and Moho depth values. The model is obtained by collecting, integrating, and interpolating reliable, published sedimentary rock thickness and Moho depth measurements in the Middle East and North Africa region. To evaluate the accuracy of the model, the 3-D gravity response of the model is calculated and compared with available observed Bouguer gravity anomalies in the region. The gravity modelling shows that the new crustal model predicts large portions of the observed Bouguer anomalies. However, in some regions, such as the Red Sea and Caspian Sea regions, where crustal structure is relatively well-determined, the residual anomalies are of the order of a few hundred milligals. Since the new crustal model results in large residual anomalies in regions where reasonably good constraints exist for the model, these large residuals cannot simply be explained by inaccuracies in the model. To analyse the cause of these residuals further we developed an isostatically compensated (Airy-type) Moho-depth model and calculated its gravity response. Isostatic gravity anomalies are in nearly perfect agreement with the observed gravity values. However, the isostatic model differs significantly from the new (3-D) crustal model. If isostasy is to be maintained, crustal and/or upper mantle lateral density variations are needed to explain the large observed gravity residuals.

Key words: basement, gravity, Middle East, Moho, North Africa

1 INTRODUCTION

Despite numerous studies that have successfully determined crustal structure in many regions on Earth, uniform compilations of these measurements at regional scales have not been realized to their full extent. As many geological and geophysical studies now require trustworthy, digital 3-D crustal models, the need to develop complete and reliable models for any part of the Earth is high. Soller *et al.* (1982) assembled one of the first compilations of global Moho and upper mantle velocity measurements. More recently, Mooney *et al.* (1998) developed a first complete global crustal model that includes sediment thickness, Moho depth, and seismic velocities at a resolution of $5^\circ \times 5^\circ$. Although this is a very low-resolution model, this data set has filled a major gap in geoscience research. Laske & Masters (1997) also developed a more detailed ($1^\circ \times 1^\circ$) global sediment thickness map. These global models provide a first-order and complete data coverage for the entire globe; however, their resolution is too coarse for regional studies. A couple of regional compilations of depth-to-Moho values have been developed for Europe based on seismic reflection and refraction data (Meissner *et al.* 1987; Geiss 1987). In this study, our main goal is to develop a regional scale crustal model that covers the Middle East and North Africa region based on data either that we have developed and/or have access to, or that are from publications that focus on local structures in the region. We then calculate the 3-D Bouguer gravity anomaly of the model and compare it with available, observed Bouguer measurements in the region. The residual anomalies are discussed with respect to their implications for isostatic compensation mechanisms in the region.

2 MODEL DEVELOPMENT

The 3-D crustal model is created by combining sediment thickness, Moho depth, and topography values nominally gridded at 25 km. It does not, however, include any physical parameters such as velocity or density at this stage. Although sufficiently detailed velocity and density information exists in some regions, the current lack of complete coverage in the region prevents us from forming reliable compilations of such physical parameters. We recommend that the model be used with globally

averaged density and or velocity information until more rigorous compilations of density and velocities are obtained. The model presented here is appropriate for regional studies and should not be utilized at local scales.

In the model development, we took full advantage of our earlier work related to building a geoscience information system for research and education (Seber *et al.* 1997, 2000), which collects and organizes regional scale geoscience data. We collected published data from the literature about the Moho depth and sedimentary rock thicknesses in the region. Fig. 1 shows the data sets that were used in our final compilation. The data sets include compilations of Soller *et al.* (1982), Mooney *et al.* (1998) and Laske & Masters (1997), as well as our own compilations in the Middle East and North Africa region. In regions where conflicting Moho and/or sediment thickness observations occur, we used the result from the more detailed data set. If no information was available, we made a judgement based on the overall tectonics of the region. For example, large portions of African crustal structure have not been studied. However, the surface boundaries of tectonic units are relatively well known and can be used to extrapolate the existing limited number of observations throughout the region.

2.1 Topography/bathymetry

The Digital Elevation Model for the crustal model is extracted from two main sources: GTOPO30, which is released by the USGS (EROS, 1996); and Smith & Sandwell's (1997) global seafloor topography. These data sets were merged and a new combined topography/bathymetry data set formed (Fig. 2).

2.2 Moho

To obtain a high-resolution gridded Moho depth map for the new crustal model, we used the data sets shown in Fig. 1. These data sets are from a variety of sources that include crustal scale refraction and reflection profiles, receiver function Moho depth estimates (Sandvol *et al.* 1998a,b), gravity modelling, and surface wave dispersion-curve inversion results. The receiver function results provide accurate Moho depths beneath 18 points in the region (Fig. 1). The majority of the Moho depth measurements in the Middle East are from 46 refraction and gravity profiles in the region (Fig. 1). The complete set of profiles and their interpretations and metadata about them are available on a web site at *http://atlas.geo.cornell.edu/htmls/fin2/figmain.html*. We digitized all these crustal cross-section interpretations and marked the Moho interfaces on each cross-section. In regions where other researchers had compiled local Moho maps, we digitized the Moho contours and added them to our pool of Moho depth values (Fig. 1). We collected contour maps for Iran, the Afar triangle, Egypt, the Aegean Sea, Greece, Italy, and the eastern Mediterranean Sea. In addition, some Moho values were digitized as points from interpretations of low-resolution refraction profiles with *PmP* measurements in northwest Africa (Fig. 1).

We also utilized Soller *et al.* (1982), Mooney *et al.* (1998), and Institute for the Physics of the Earth (IPE) (Kunin 1987) Moho values in regions outside the Middle East and North Africa to obtain a more complete coverage of the entire area. In regions where the Moho depth is prone to sudden changes, such as at continental margins and mid-ocean ridges, and no observational data are available, we opted to assign Moho depths (pseudo-Moho) based on tectonic knowledge and global averages. Using a bathymetry map with a resolution of 3 km, we outlined the edge of the continental shelf and assigned a Moho thickness of 25 km to these contours. The 25 km Moho depth was chosen to approximate the crustal thinning from the continental regions to oceanic regions. Similarly, we assigned a crustal thickness of 5 km along the mid-ocean ridges. Finally, the entire compilation was gridded using an iterative finite difference interpolation technique developed for spatial analysis of Geographic Information System (GIS) data sets using ArcInfo© GIS software. The final gridded Moho depth map is shown in Fig. 2. The Moho depth values are from sea level.

2.3 Sediment thickness

To obtain the sediment thickness values for the new crustal model, we merged our database of depth to metamorphic basement shown in Fig. 1 with that of Laske & Masters (1997). Our basement depth values cover only the continental regions in the Middle East and North Africa, and come from crustal scale refraction and reflection profiles, drill-hole measurements, and gravity modelling. In addition to the crustal scale profiles shown in Fig. 1, the basement depth values for most of the African continent were also digitized from a map of the geology of Africa (Yarmolyuk & Kuznetsov 1977). In Algeria and Libya, where there are high-resolution basement maps available, we digitized those maps and replaced the values of the lower-resolution basement map. In regions where the basement crops out, we used the highest-resolution publicly available topography values to represent a continuous surface for the basement structure.

Finally, this compilation was also gridded, and the topographic/bathymetric grid was added to the sediment thickness grid, and the final depth-to-basement values from the sea level were obtained (Fig. 2).

3 THREE-DIMENSIONAL GRAVITY MODELLING AND TECTONIC IMPLICATIONS

3.1 Method

The model developed above provides a rare opportunity to model simultaneously the gravity effects of diverse tectonic regions in the Middle East and North Africa, namely regions of subduction, rifting, continental collision and transform faulting, as well as platform and shield areas. We chose to calculate the 3-D gravity anomaly by converting our model into prisms, and calculated the gravity effect of these prisms individually (Fig. 3). By summing the resultant anomalies we obtained a complete gravity response of the model. Plouff (1976) derived the formula to calculate the 3-D gravity anomalies of a prism with arbitrary dimensions (Fig. 3). This is computationally challenging, but an accurate technique for calculating the gravity anomalies of any arbitrarily shaped 3-D model. By making the widths of the prisms small, irregularly shaped models can be approximated at fine scales, and 3-D gravity anomalies can be computed. We have tested this approach against well-established 2-D gravity modelling programs, and the results show that variations in calculated anomalies are of the order of a few milligals. Since our model is based on 25×25 km cell

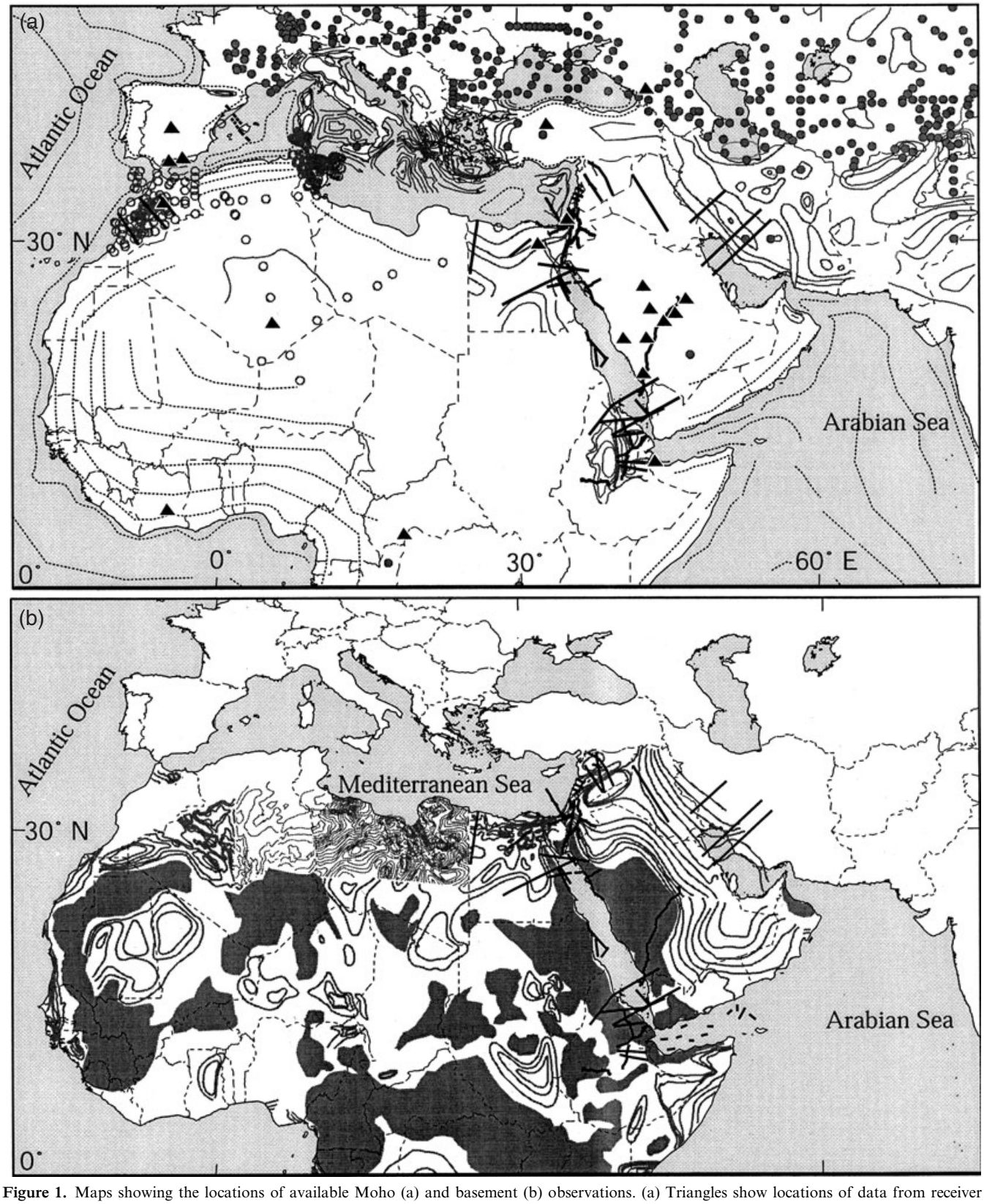

Figure 1. Maps showing the locations of available Moho (a) and basement (b) observations. (a) Triangles show locations of data from receiver function studies, thick lines are refraction and gravity interpretations, contours represent various digitized Moho maps, grey circles represent data from Soller *et al.* (1982), and open circles are values obtained from low-resolution seismic/gravity interpretations. Dashed lines represent depth-to-Moho values interpreted based on the tectonics of the regions. (b) Black lines represent seismic/gravity measurements, grey contours are from various sediment thickness maps, and grey areas represent basement outcrops.

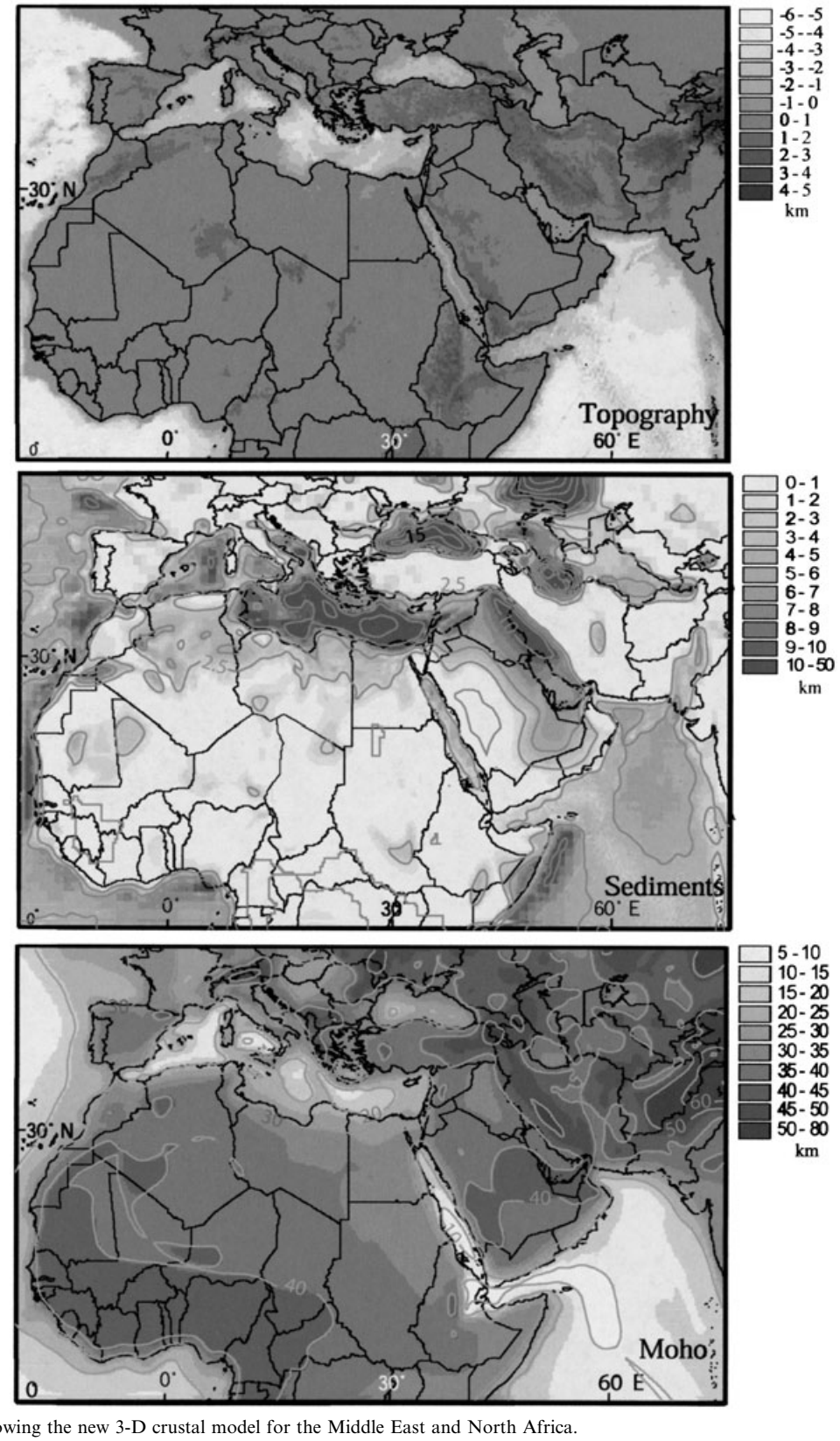

Figure 2. Maps showing the new 3-D crustal model for the Middle East and North Africa.

sizes, each cell in our model was a prism with horizontal dimensions of 25×25 km and the corresponding depth value (Moho or basement) as the third dimension. The tops of the prisms were fixed at sea level.

In order to calculate the regional gravity anomaly of our model we have to assign an average density contrast for the sediment–basement and crust–upper mantle boundaries. Since our goal here is to calculate and compare regional scale gravity

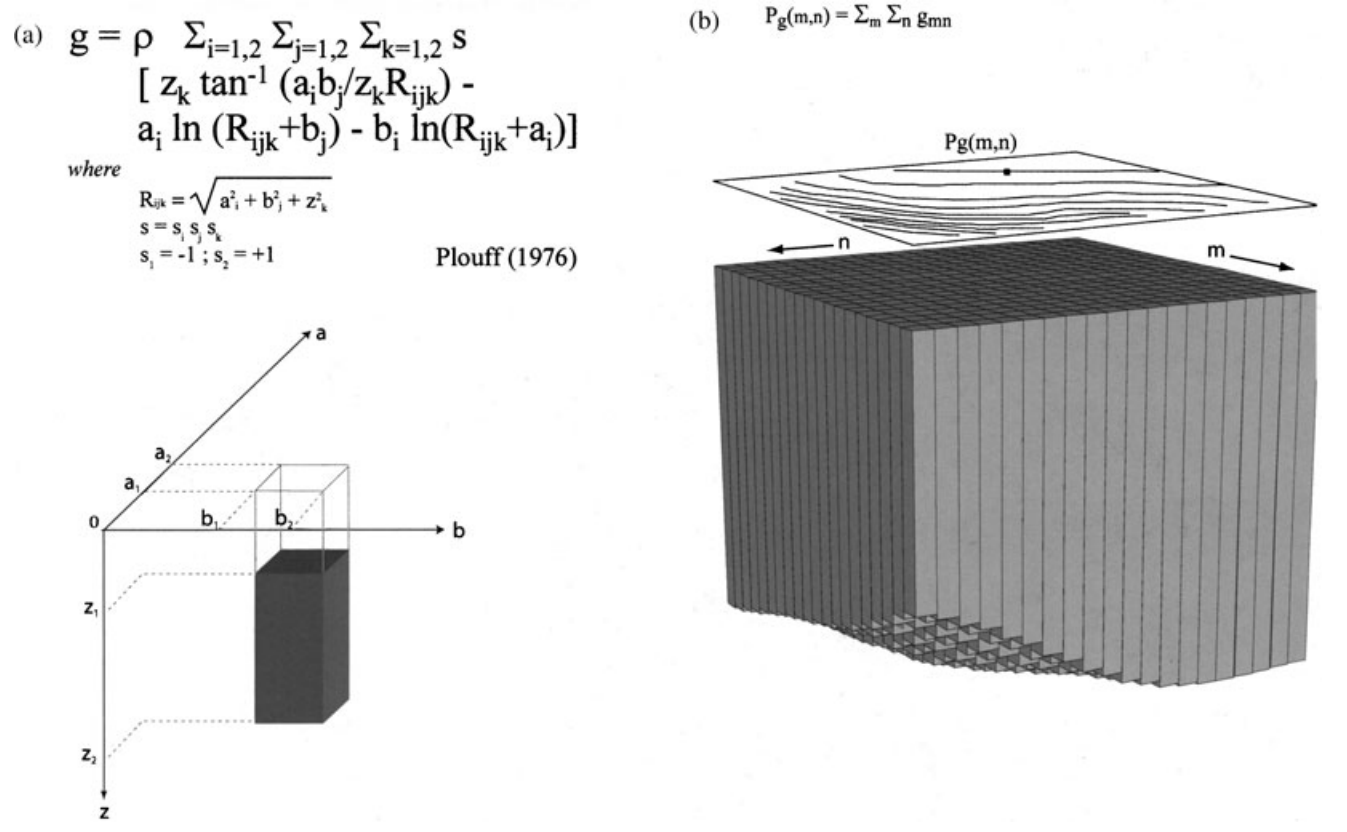

Figure 3. Calculation of gravity anomalies for our 3-D crustal model. (a) The gravity anomaly of a prism at any given point can be calculated using the formula provided by Plouff (1976). (b) The total gravity anomaly at a given point $P_g(m, n)$ can then be calculated by taking the sum of gravity anomalies of all prisms in the model.

anomalies and our model does not include comprehensive density information, we opted to use globally averaged density values in our gravity calculations. We are able to use simplified average values because we only seek first-order gravity anomalies at a regional scale. Practically, we are making an assumption that density values within the sediments, crust and sub-Moho do not change significantly. This assumption is more valid for the Moho than it is for the sediments. Undoubtedly, densities within sediments vary significantly. However, since we are interested in the whole-basin gravity response, not in local density variations in sedimentary basins, the approach of using a uniform density value should provide a first-order result and be sufficient for our tests. The model and the gravity algorithm, however, are designed such that, if detailed density values become available, more accurate gravity anomalies can be calculated without any changes to the system.

We chose a density contrast of 0.4 g cm^{-3} between the lower crust and uppermost mantle, which is a value comparable to global averages and previous studies (Christensen & Mooney 1995). In deep oceanic areas (water depth >3000 m), where typical oceanic crust is thought to exist, we reduced the density contrast to 0.3 g cm^{-3} to accommodate the denser oceanic crust. To evaluate the effects of the ambiguity of density values we also utilized crust–mantle density contrasts of 0.5 and 0.3 g cm^{-3}. We found that the density contrast of 0.5 g cm^{-3} was too large and the calculated gravity maximum and minimum values in the region were significantly larger than those of the observed minimum and maximum. Similarly, we found that the value of 0.3 g cm^{-3} did not provide a satisfactory fit to the gravity anomalies: the range between the gravity maximum and minimum in the calculated values was smaller than the observed anomalies. The density contrast between the sediments and surrounding metamorphic basement rocks was chosen as 0.3 g cm^{-3}. To evaluate this value, we made several tests using sedimentary–basement rock density contrasts of 0.2 and 0.4 g cm^{-3}. The resultant anomalies were within a few tens of milligals from our preferred density contrast of 0.3 g cm^{-3}.

3.2 Observed gravity data

Unfortunately, a complete coverage of observed gravity values in the region is not available. The most complete gravity data coverage comes from the National Imagery and Mapping Agency (NIMA) gravity database. This data set covers large parts of the region. However, to supplement these data we digitized Bouguer gravity maps for Turkey and Syria. The Turkish Bouguer gravity values were obtained from Ates *et al.* (1999), and the Syria gravity values were obtained from the Gravity Maps of Syria (BEICIP report 1975). All these data sets were combined and gridded at 10 km intervals.

3.3 Results

Fig. 4 shows the contour maps of the calculated Bouguer gravity anomalies displayed over the observed Bouguer gravity map. Overall, the shapes of the observed and calculated values

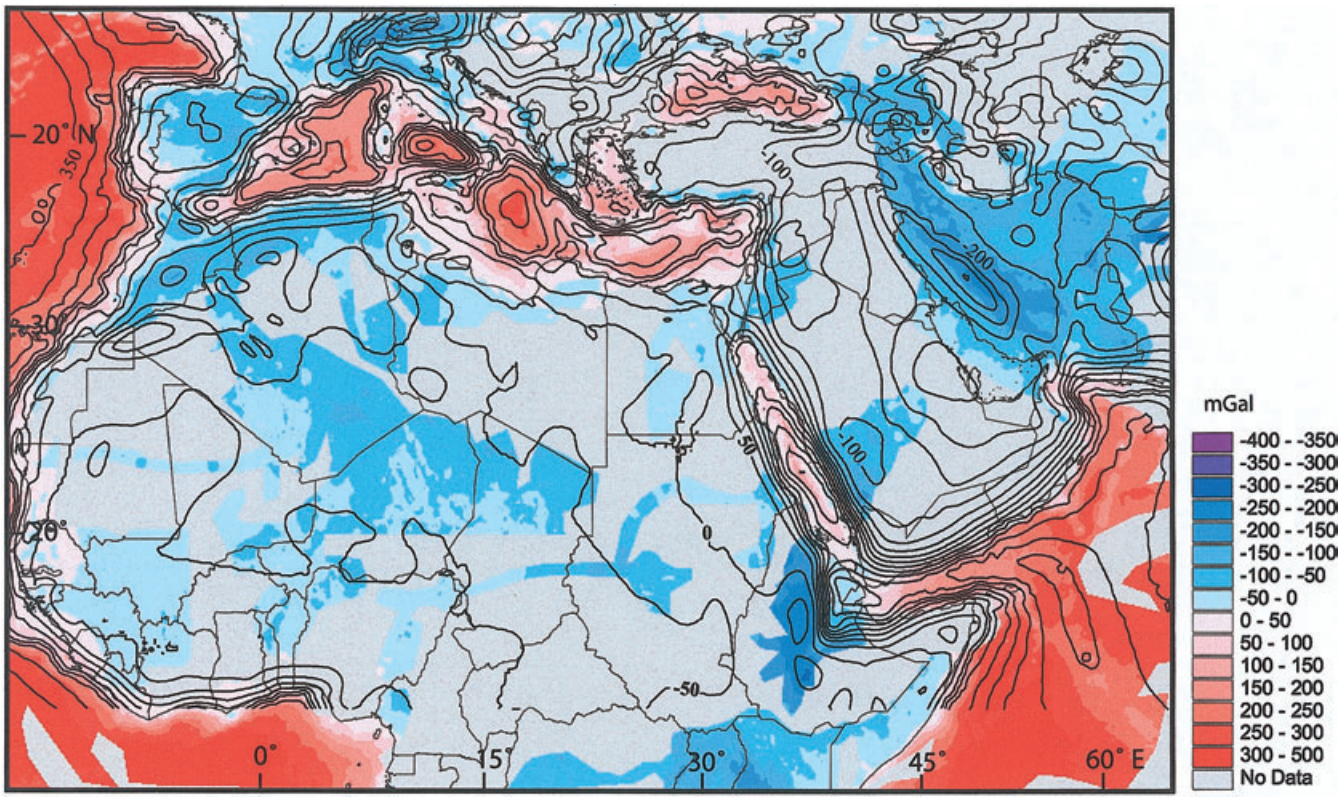

Figure 4. Map showing a comparison of observed (coloured image) and calculated (contour) Bouguer gravity values. The contour interval is 50 mGal. The calculated values are the gravity response of the crustal model shown in Fig. 2.

correlate well. However, in some regions the magnitudes of the anomalies are quite different. Fig. 5 shows the residual anomalies obtained by subtracting the observed gravity values from the calculated ones. This residual anomaly map shows that large gravity residual anomalies are obtained mainly in five distinct regions: the Red Sea, northern Arabia, the Caspian Sea and parts of Eurasia, the western Mediterranean, and western Africa. Except for western Africa, substantial amounts of data

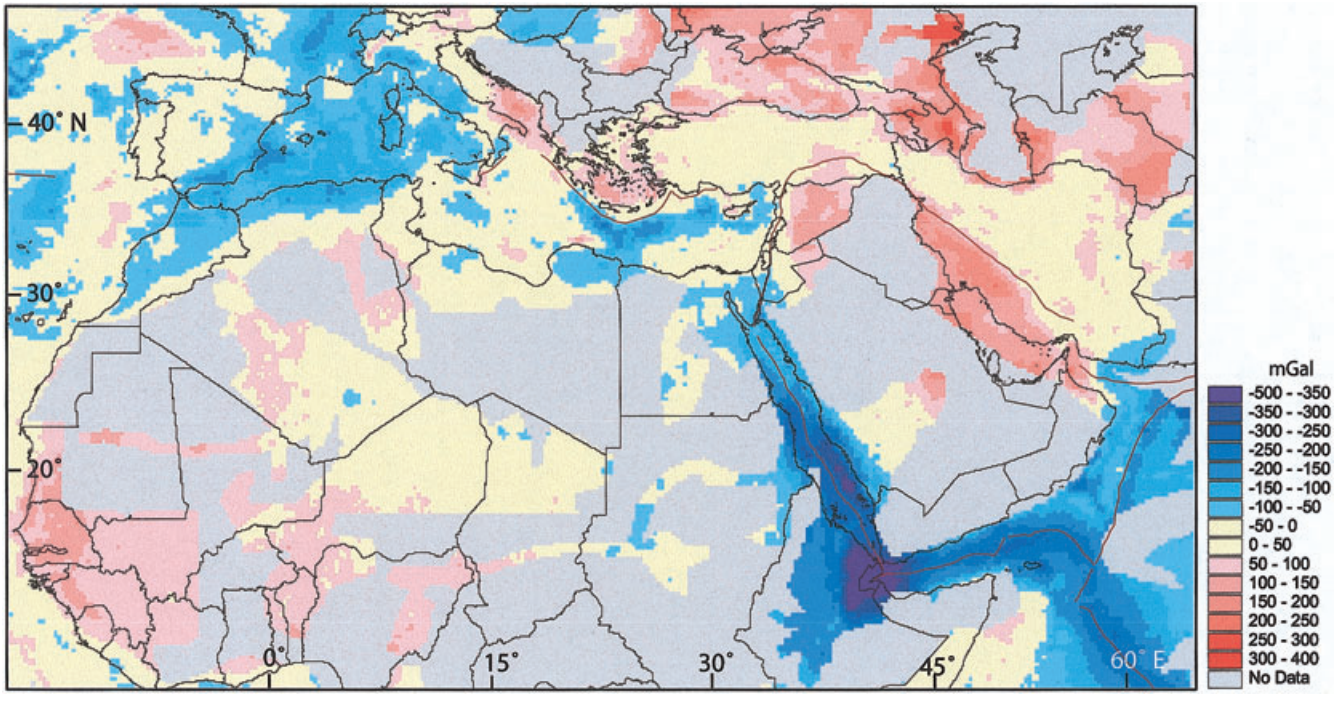

Figure 5. Map of residual (observed–calculated) gravity anomalies. Blue tones represent regions where the model predicts much higher gravity anomalies, and pink tones represent regions where the model predicts lower anomalies compared to observed gravity values. Current plate boundaries are shown by the red lines.

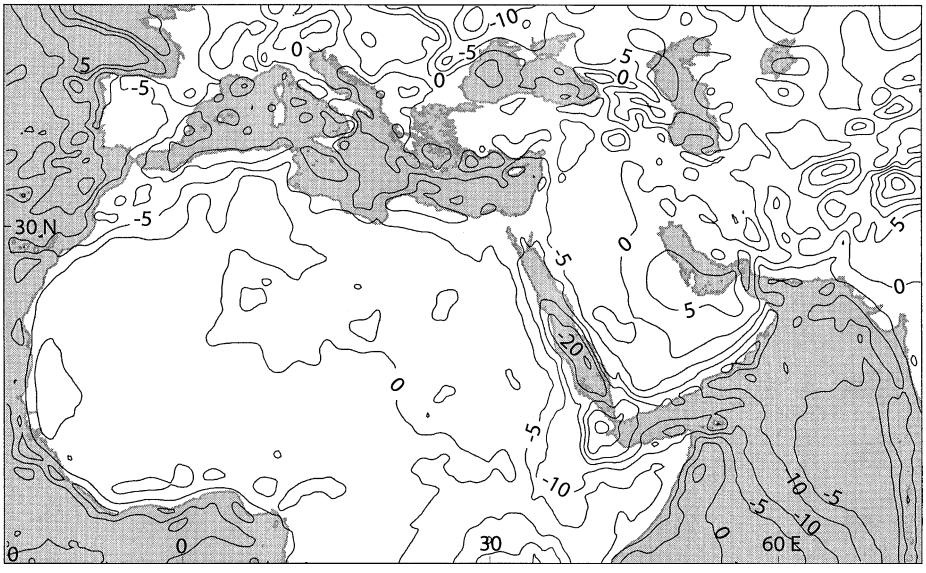

Figure 6. Map showing the difference in Moho depth between the observed Moho values and the isostatic Moho values. The largest difference (of about 20 km) is observed in the Red Sea region.

exist to constrain the crustal structure in these regions. Even though the depth to Moho and basement values in these regions include some errors, the magnitudes of the residual anomalies are too large to simply explain these residuals by inaccuracies in the model. Sources other than sediment and/or Moho depth need to be investigated as potential causes of these residual anomalies.

Before pursuing a detailed analysis of these residual anomalies, we performed isostatic gravity modelling to determine whether or not the region is isostatically compensated. To do this, we assumed an Airy-type isostatic mechanism, used the topography averaged at 25 km to estimate the load, and determined the corresponding isostatic Moho depth variations (Fig. 6). The base Moho thickness was chosen to be 35 km. We used a 0.4 g cm^{-3} density difference between the lower crust and uppermost mantle, as in our 3-D gravity calculations. Calculated gravity values for the isostatically compensated Moho model show a remarkable match with the observed gravity values (Fig. 7). The only significant isostatic residual anomaly is found in the southern part of the Aegean subduction zone, where isostatic residuals are larger than 50 mGal. The overall correlation implies that the Middle East and North Africa region is in nearly complete isostatic equilibrium. However, based on our crustal model, we can clearly state that the compensation mechanism in the region is not a simple Airy mechanism.

Fig. 5 shows that the largest residual anomaly is a negative in the Red Sea region and its surroundings. Since we have

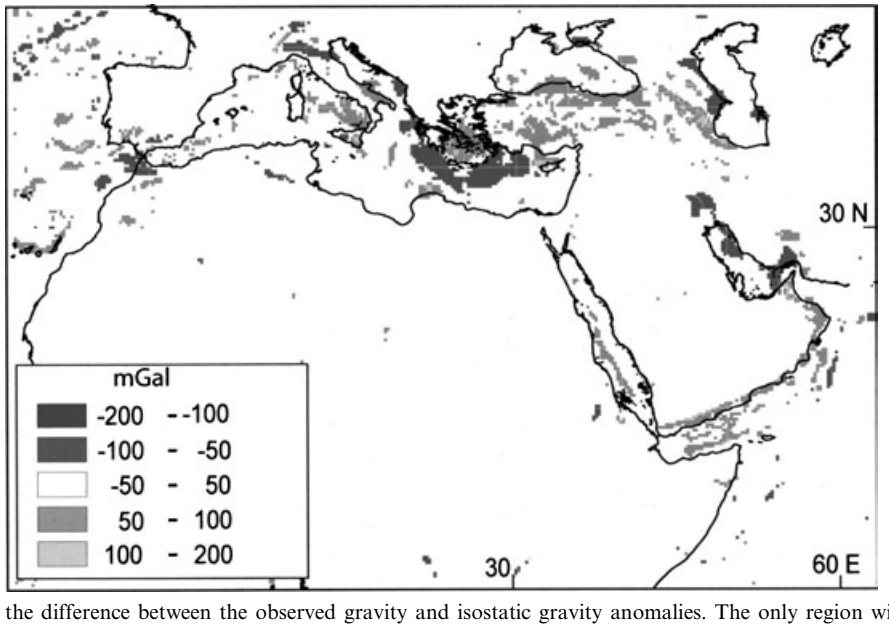

Figure 7. Map showing the difference between the observed gravity and isostatic gravity anomalies. The only region with a significant isostatic residual anomaly is in the Aegean Sea and its surrounding. The remaining areas show very minor isostatic residual anomalies, implying that the region is under isostatic compansation.

numerous observations of Moho and sediment thickness in the region, we cannot simply attribute this large anomaly to errors in the crustal model. Since the region is a young rift zone, where the lithosphere has significant lateral variations in thickness and density and where asthenospheric material resides at shallower levels (Cochran 1983), we interpret this negative residual anomaly as primarily due to rising hotter upper mantle material. This anomaly extends into Africa along the East African rift system. Unfortunately, the lack of observed gravity data in the region prevents us from mapping the lateral extent of this low-density material.

The second large residual anomaly is located in the Arabian plate. A large positive residual anomaly in the northern and eastern portions of the Arabian plate correlates well with the current plate boundaries. This anomaly cannot be explained by possible errors in the model either, as we have reasonably good observations in this region. Two possible explanations exist. The first one is to assume that higher-density material beneath Arabia resides at subcrustal levels (i.e. a denser mantle lid). The alternative interpretation is that the source of the positive residual anomaly is in the crust (i.e. a denser crust). Since the boundary of the anomaly matches well with the suture zones, and the crust in neighbouring regions (Iran and Turkey) is hotter as evidenced by young volcanism and high attenuation (e.g. Gok *et al.* 2000; Sandvol *et al.* 2001), the latter interpretation is more favourable. However, a detailed study needs to be conducted in order to determine the real cause of this anomaly.

The positive residual anomalies in the Caspian and Black seas as well as in Turkmenistan are interpreted to be a result of higher-density mantle lithosphere. This interpretation is based on the fact that strong structural variations in the crust are likely to be the source of this relatively uniform but widespread residual anomaly. The sediment thickness in the southern Caspian Sea is estimated to be about 20 km (Fig. 2). In order to obtain such high gravity values above this region, higher-density material must reside in the lower crust and/or in the upper mantle. Earlier studies have also indicated that this part of the Eurasian continent is underlain by a denser mantle lithosphere (Artemjev *et al.* 1994). Combining these two observations, we conclude that higher-density material in the uppermost mantle is the likely candidate for the cause of this anomaly.

The other large negative residual anomaly is located in the western Mediterranean Sea. A widespread anomaly of -150 to -100 mGal covers the entire western Mediterranean region. This part of the Mediterranean Sea is a relatively young region that has undergone several recent episodes of extensional tectonics and volcanism. The main extensional regions include the Tyrrhenian Sea, the Apennines, Balearic Sea, and the Alboran Sea areas. It is also known that in this region the uppermost mantle seismic speeds are very low (7.6–7.8 km s^{-1} for P_n velocities) and seismic attenuation is quite high (e.g. Calvert *et al.* 2000). Hoernle *et al.* (1995) suggested that the western Mediterranean region is underlain by upwelling mantle at the base of the lithosphere. These observations suggest that the source of this residual is probably in the uppermost mantle.

We also find a large positive residual anomaly (about 50–150 mGal) in western Africa. It is much harder to speculate on the source of this anomaly, as our crustal structure in the region is not well constrained. Only a few points constrain the model in the region. However, if the calculated residual anomaly is not a function of model artefacts, we might speculate that, since the location of the anomaly corresponds to the craton areas of west Africa, the positive residual anomaly might indicate the higher-density craton in the region. Until more information about the crustal structure in this region is obtained, the origin and nature of this anomaly will remain doubtful.

4 CONCLUSIONS

The compilation of Moho and sediment thickness values in the Middle East and North Africa region has allowed the construction of the first detailed regional scale 3-D crustal model for the region. Although portions of this model need to be improved, it will be useful in various geological and geophysical studies in the region. Comparison of the 3-D gravity anomalies calculated based on this new crustal model with the observed gravity anomalies provides new insights into the geodynamic processes in the region. Two large negative residual anomalies (Red Sea and western Mediterranean) and two large positive residual anomalies (northern Arabia and southern Eurasia) have been mapped based on the model response. Although the region appears to be in nearly complete isostatic equilibrium, the compensation mechanism is not only of an Airy type. We conclude that regional scale lateral density variations in the crust and in the uppermost mantle play a major role in this equilibrium.

ACKNOWLEDGMENTS

The work was funded by the Department of Energy, Cooperative Agreement DE-FC04–99AL66045 and the Department of Defense grant DSWA01-97-1-0006. We thank G. Brew for helping us to evaluate the code used in the gravity calculations, and D. Turcotte for reading an earlier draft of this manuscript and for providing comments on the results. We also thank the two reviewers, R. Keller and E. Fluh, for their useful comments and suggestions.

REFERENCES

Artemjev, M.E. & Kaban, M.K., 1994. Density inhomogeneities, isostasy and flexural rigidity of the lithosphere in the transcaspian region, in *Dynamics of Extensional Basin Formation and Inversion,* eds Cloetingh, S., Eldholm, O., Larsen, B.T., Gabrielsen, R. & Sassi, W., *Tectonophysics*, **240,** 281–297.

Ates, A., Kearney, P. & Tufan, S., 1999. New gravity and magnetic anomaly of Turkey, *Geophys J. Int.,* **136,** 499–502.

BEICIP Report, 1975. *Gravity Maps of Syria: Damascus, Syria,* Bureau d'Etudes Industrielles et de Cooperation de l'Institut Francais du Petrole, Damascus, Syria.

Calvert, A., Sandvol, E., Seber, D., Barazangi, M., Vidal, F., Alguacil, G. & Jabour, N., 2000. Propagation of regional seismic phases (Lg and Sn) and Pn velocity structure along the Africa–Iberia plate boundary zone: tectonic implications, *Geophys J. Int.,* **142,** 384–408.

Christensen, N. & Mooney, W., 1995. Seismic velocity structure and composition of the continental crust; a global view, *J. geophys Res.,* **100,** 9761–9788.

Cochran, J., 1983. A model for development of Red Sea, *Am. Assoc. Petrol. Geol. Bull.,* **67,** 41–69.

EROS (Earth Resources Observation Systems), Data Center (EDC), 1996. GTOPO30 (a Digital Elevation Model), United States Geological Survey (USGS), www.usgs.gov.

Geiss, E., 1987. A new compilation of crustal thickness data for the Mediterranean area, *Ann. Geophys.,* **5,** 623–630.

Gok, R., Turkelli, N., Sandvol, E., Seber, D. & Barazangi, M., 2000. Regional wave propagation in Turkey and surrounding regions, *Geophys Res. Lett.,* **27,** 429–432.

Hoernle, K., Zhang, Y. & Grabham, D., 1995. Seismic and geochemical evidence for large-scale mantle upwelling beneath the eastern Atlantic and western Europe, *Nature,* **374,** 34–38.

Kunin, N., 1987. *Map of Depth to Moho, Moscow, Russia, 1: 15,000,000 scale,* 2 Sheets, Institute of Physics of the Earth, Moscow, Russia.

Laske, G. & Masters, G., 1997. A global digital map of sediment thickness, *EOS, Trans. Am. geophys. Un.,* **78,** F483.

Meissner, R., Wever, T. & Fluh, E.R., 1987. The Moho in Europe—Implications for crustal development, *Ann. Geophys.,* **5B,** 357–364.

Mooney, W.D., Laske, G. & Masters, T.G., 1998. CRUST 5.1: a global crustal model at $5^\circ \times 5^\circ$, *J. geophys Res.,* **103,** 727–747.

Plouff, D., 1976. Gravity and magnetic fields of polygonal prisms and application to magnetic terrain corrections, *Geophysics,* **41,** 727–741.

Sandvol, E.D., Seber, D., Calvert, A. & Barazangi, M., 1998a. Grid search modeling of receiver functions: implications for crustal structure in the Middle East and North Africa, *J. geophys Res.,* **103,** 26 899–26 917.

Sandvol, E., Seber, D., Barazangi, M., Vernon, F., Mellors, R. & Al-Amri, A., 1998b. Lithospheric seismic velocity discontinuities beneath the Arabian Shield, *Geophys Res. Lett.,* **25,** 2873–2876.

Sandvol, E., Al-Damegh, K., Calvert, A., Seber, D., Barazangi, M., Muhamed, R., Gok, R., Turkelli, N. & Gurbuz, C., 2001. Tomographic imaging of Lg and Sn propogation in the Middle East, *Pure appl. Geophys.,* **158,** 1121–1163.

Seber, D., Vallve, M., Sandvol, E., Steer, D. & Barazangi, M., 1997. Geographic information systems (GIS) in earth sciences: An application to the Middle East region, *GSA Today,* **7,** 1–6.

Seber, D., Steer, D., Sandvol, E., Sandvol, C., Brindisi, C. & Barazangi, M., 2000. Design and development of information systems for the geosciences: An application to the Middle East, *Geoarabia,* **5,** 269–296.

Smith, W.H.F. & Sandwell, D., 1997. Global seafloor topography from satellite altimetry and ship depth soundings, *Science,* **277** (5334), 1956–1962.

Soller, D.R., Ray, R.D. & Brown, R.D., 1982. A new global crustal thickness map, *Tectonics,* **1,** 125–149.

Yarmolyuk, V.A. & Kuznetsov, Y.Y., 1977. *Geological Map of Africa, 1: 5,000,000 scale,* 2 Sheets, Ministry of Geology of the USSR, Moscow, Russia.